

## Measurement of the apparent diffusion coefficient in the liver: is it a reliable index for hepatic disease diagnosis?

Katsuhiro Nasu · Yoshifumi Kuroki · Ryuzo Sekiguchi  
Toshiki Kazama · Hiroto Nakajima

Received: April 25, 2005 / Accepted: February 20, 2006  
© Japan Radiological Society 2006

### Abstract

**Purpose.** The aim of this study was to determine the validity of the hepatic apparent diffusion coefficient (ADC) measurement. The influence of differences in measured location and administration of Buscopan (hyoscine butylbromide) for ADC were assessed.

**Materials and methods.** SENSE-DWI ( $b = 0, 500$ ) was obtained before and after Buscopan administration to 30 patients suspected of having a liver tumor. In this sequence, respiration gating was employed, but cardiac triggering was not. ADC measurement was performed in the hepatic parenchyma of both right and left lobes in selected slices. A statistical analysis was performed to estimate the correlation among ADC, measured location, Buscopan, and pulse rate. The images were visually evaluated to categorize the subcardiac signal loss in the left lobe.

**Results.** The ADC showed higher values in the left lobe than in the right lobe in both pre- and postloaded studies ( $P < 0.001$ ). In a comparison between ADCs in the pre- and postloaded studies, the differences were not

significant in the left lobe ( $P = 0.93$ ) or the right lobe ( $P = 0.41$ ). No correlation was noted between ADCs and the pulse rate. Visual evaluation revealed that the subcardiac signal loss was more prominent in the postloaded study.

**Conclusion.** ADC measurement of the left hepatic lobe was far more incorrect than that of the right lobe if cardiac gating was not employed. The administration of Buscopan worsened the image quality of the left lobe and made visual evaluation difficult.

**Key words** SENSE-DWI · ADC · Liver · Cardiac pulsation

### Introduction

Since the adoption of parallel imaging techniques such as sensitivity encoding (SENSE), diffusion-weighted imaging (DWI) is increasingly being employed to image body malignancies.<sup>1–3</sup> The usefulness of diffusion-weighted single shot echo planar imaging with SENSE (SENSE-DWI) when screening for hepatic metastasis is particularly outstanding.<sup>4</sup>

On the other hand, DWI is known to be extremely sensitive to motion in subjects.<sup>5–7</sup> We therefore doubt the correctness of DWI measurements when the liver shows significant physiological motion. During clinical image interpretation, we often encountered a signal drop in the lateral segment, assumed to be due to cardiac pulsation (hereinafter termed subcardiac signal loss). We also observed that this phenomenon became more prominent after the administration of butyl scopolamine (Buscopan; Nihon Boehringer Ingelheim, Kawanishi, Japan).

K Nasu (✉) · Y. Kuroki · R. Sekiguchi  
National Cancer Center Hospital East, 6-5-1 Kashiwanoha,  
Kashiwa, Chiba 277-8577, Japan  
Tel. +81-4-7133-1111; Fax +81-4-7131-4724  
e-mail: kanasu@east.ncc.go.jp

T. Kazama  
Department of Radiology, Chiba University, School of  
Medicine, Chiba, Japan

H. Nakajima  
Department of Radiology, Yamanashi University School of  
Medicine, Yamanashi, Japan

This article was presented at the Japan Radiological Society meeting in 2005.

In this article, we assess the influences of apparent diffusion coefficient (ADC) measurement of hepatic parenchyma by employing differences in the measured area and administration of Buscopan. We also discuss the clinical propriety of ADC measurement in patients with hepatic DWI.

## Materials and methods

### Patient group

MR imaging of the liver was performed in 63 patients during October 2004 at the National Cancer Center Hospital East. Among them, the patients who did not have any liver dysfunction in their blood sample data and did not have any contraindications for Buscopan were selected for the study. This study was approved by our institutional review board, and informed consent was obtained from all the patients. The group comprised 15 men and 15 women ranging from 38 to 78 years old (mean 62.1 years). The aim of the magnetic resonance (MR) examination of each patient was the following: clinical staging of extrahepatic malignancy (15 cases), evaluation of hepatic metastasis extent before surgery (11 cases), and diagnosis of hepatic hemangioma (4 cases). The only preparation before the examination was an 8-h fast. Existing daily drugs were not stopped before the examination.

### Imaging protocols

The MR apparatuses we used were a Gyroscan Intera Master 1.5T and a SENSE body coil (Philips Medical, Best and Heeren, The Netherlands). These apparatuses and the sequences described below are all commercially available and were purchased from the manufacturer as Release 9. The following imaging sequence was obtained before and after administration of Buscopan: diffusion-weighted single-shot echo planar imaging with SENSE (SENSE-DWI) [TR/TE = 1600/73, b-factor = 0, 500 s/mm<sup>2</sup>, spectral presaturation with inversion recovery (SPIR) for fat suppression, matrix size 256 × 97, half scan factor 0.693, reduction factor of SENSE 2.0, field of view (FOV) 35 × 28 cm, number of excitations 5, slice thickness/gap 7 mm/1 mm, 22 axial slices, respiration trigger, mean actual scan time 2–3 min]. This is the sequence used in our institution. The imaging parameters were determined to balance the image quality and diffusion contrast. Therefore, this sequence was not optimized to measure the ADC.

Motion-probing gradient (MPG) pulses were placed along the three (X, Y, Z) axes. The image series in which

the MPG pulse was placed along each direction were called DWI-X, DWI-Y, and DWI-Z, respectively. During image interpretation, we used only the trace images synthesized from the three images in which the MPG pulses were placed in each direction. The slice thickness, gap, and FOV were occasionally changed depending on the size of the liver so the whole liver was covered.

Buscopan (20 mg per body, diluted threefold with physiological saline) was administered intravenously after the preloaded images had been obtained. Drug injection was performed using a power injector (Sonic Shot 50; Nemoto Kyorindo, Tokyo, Japan) and took precisely 30 s. During the examination, pulse rates were constantly monitored using a peripheral pulse sensor linked to the MR apparatus. The postloaded images were started after the pulse rate reached a plateau. The mean pulse rates during each image acquisition were obtained by averaging the pulse rates at the beginning and the end of each image acquisition.

### Imaging analysis

Based on mutual agreement, two diagnostic radiologists selected slices for evaluation from the obtained images. Three contiguous slices were chosen for evaluation from each patient; the slices were close to the diaphragm, and no partial volume effects were observed in either the right or the left lobe. The reason only three slices were chosen was the individual differences in the craniocaudal length of the lateral segment. In the thinnest lateral segment, only three slices could be selected. To match the anatomical slice levels of selected images between the pre- and postloaded images, respiratory misregistration was corrected by the two aforementioned radiologists based on mutual agreement.

The ADCs of hepatic parenchyma were measured in both the right and left lobe on ADC maps generated by the two-point method in each selected slice.<sup>8</sup> The methods used for generating the region of interest (ROI) are described below.

1. Initially, the two aforementioned radiologists compared DWI-X, DWI-Y, and DWI-Z with T2-EPI (b = 0) and confirmed the presence or absence of anatomical misregistration. If the misregistration was verified, the patient was excluded from this study.
2. ROIs generated on T2-EPI were copied and pasted onto ADC maps of the pre- and postloaded studies. (For this procedure, we used the “copy to temp/copy from temp” function that was included in the MR apparatus.)
3. To avoid the influence of the partial volume effect, a 1-cm margin of the liver was excluded from the ROI.

4. The ROI was set as large as possible in each lobe of each slice. Thin structures (containing lesions) measuring less than 1 cm were included in the ROI. However, large structures measuring 1 cm or more were excluded.

The aforementioned radiologists performed a visual evaluation of each selected image based on mutual agreement. They classified the grades of subcardiac signal loss into three categories according to the following criteria.

Grade 1: no subcardiac signal loss in the left lobe.

Grade 2: slight subcardiac signal loss partially or generally seen in the left lobe; however, the margin of the left lobe could be clearly identified.

Grade 3: significant subcardiac signal loss partially or generally seen in the left lobe, with the margin of the left lobe not observable due to the artifact.

### Statistical analysis

The obtained ADCs were divided into four groups: (1) ADCs of the left lobe in the preloaded study; (2) ADCs of the right lobe in the pre-loaded study; (3) ADCs of the left lobe in the pos-loaded study; and (4) ADCs of the right lobe in the postloaded study. Statistical analyses were made between the corresponding slices of (1) and (2), (3) and (4), (1) and (3), and (2) and (4) using the Wilcoxon's paired signed rank test.

Mean ADCs of right and left lobes were obtained by averaging the ADCs of the selected slices from each patient in each study. These mean ADCs represented the ADC of each hepatic lobe of each patient at each pulse rate, and the correlations between these mean ADCs and pulse rates were calculated by univariate linear regression analysis and expressed using Pearson's correlation coefficient. The following four issues were evaluated: (1) mean ADCs of the left lobe in the preloaded study and pulse rate, (2) mean ADCs of the right lobe in the preloaded study and pulse rate, (3) mean ADCs of the left lobe in the postloaded study and pulse rate, and (4) mean ADCs of the right lobe in the postloaded study and pulse rate.

As can be easily surmised, the ADC measurements of the upper abdominal organs were inaccurate, and the hepatic ADCs were scattered not only among patients but also among slices from a single patient. Thus, the interslice scattering of ADCs in each lobe and each study was evaluated. The values between the maximum and minimum ADC of the each hepatic lobe were calculated and compared for each study and each patient. This interslice ADC value was statistically evaluated using Wilcoxon's paired signed rank test.

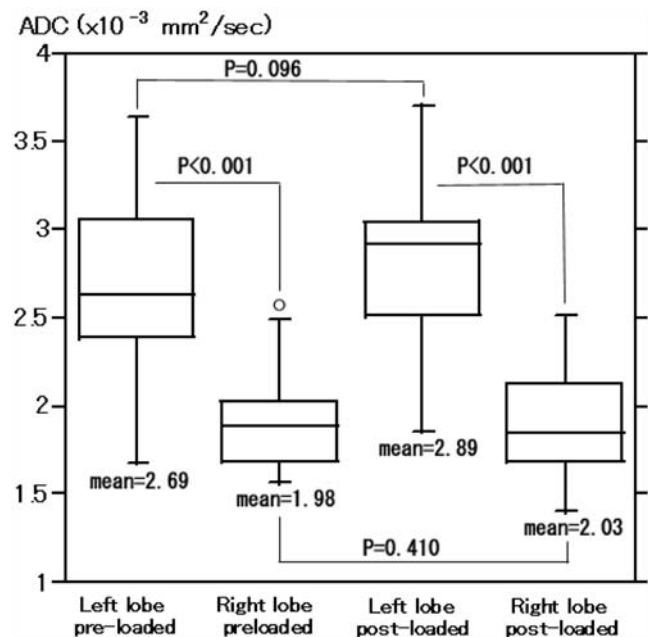


**Fig. 1.** Correlation among apparent diffusion coefficient (ADC), measured location, and Buscopan administration. The ADCs of the left lobe show statistically higher values than those of the right lobe both in the preloaded and postloaded study ( $P < 0.001$ ). However, the statistical analysis reveals that the differences between the preloaded ADCs and postloaded ADCs in both left and right lobes were not significant ( $P = 0.096$  and  $P = 410$ , respectively)

Concerning the visual evaluation, the Wilcoxon paired signed rank test was used to assess the difference in the corresponding grades of the pre- and postloaded studies.

The StatMate III package for Windows was used to carry out the aforementioned analyses.

### Results

In the comparison of DWI-X, DWI-Y, DWI-Z, and T2-EPI, there was no overt misregistration of the anatomical slice level for each patient. Therefore, all candidates could be included into the study. The pulse rates of the preloaded study ranged from 50 to 101/min (mean 68.9/min), and those of the postloaded study ranged from 76 to 125/min (mean 103.0/min).

The ADC measurement results are summarized in Fig. 1. The ADCs (mean  $\pm$  SD ( $\times 10^{-3}$  mm<sup>2</sup>/s) of groups 1–4 mentioned earlier were  $2.69 \pm 0.20$  (left lobe, preloaded),  $1.98 \pm 0.40$  (right lobe, preloaded),  $2.89 \pm 0.46$  (left lobe, postloaded), and  $2.03 \pm 0.44$  (right lobe, postloaded). The statistical analysis revealed significant differences between the preloaded ADCs of the left lobe and the right lobe ( $P < 0.001$ ) and between the

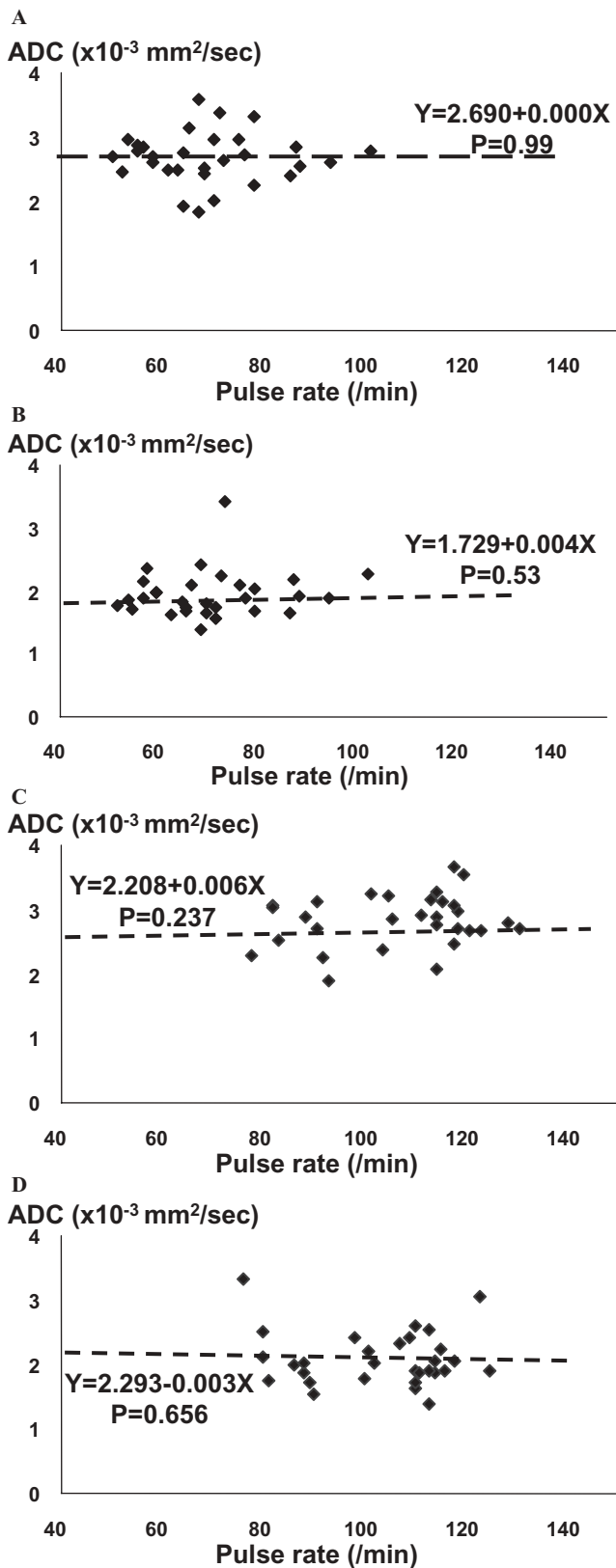


**Fig. 2.** Correlation between mean ADCs and pulse rates of each lobe in the pre- and postloaded study. The univariate linear regression analysis and Pearson’s correlation coefficient reveal that the mean ADCs of the left and right lobes in each patient do not show a clear correlation with the corresponding pulse rates

**Table 1.** Interslice remainder of ADC in each lobe and each study

Condition	Left lobe	Right lobe
Preloaded	0.44 ± 0.27	0.25 ± 0.19
Postloaded	0.48 ± 0.22	0.27 ± 0.19

Results are give as the number × 10<sup>-3</sup> mm<sup>2</sup>/s  
 \* *P* = 0.006; \*\* *P* < 0.001; \*\*\* *P* = 0.19; \*\*\*\* *P* = 0.44

**Table 2.** Visual evaluation of subcardiac signal loss in the left lobe

Condition	Grade 1	Grade 2	Grade 3
Preloaded	33	45	12
Postloaded	11	38	41

*P* < 0.001

postloaded ADCs of the left lobe and the right lobe (*P* < 0.001). The differences between the right lobe ADCs in the pre- and postloaded studies and between the left lobe ADCs in the pre- and postloaded studies were not statistically significant (*P* = 0.41 and *P* = 0.093, respectively). Moreover, the mean ADCs of the left and right lobes in each patient did not show a clear correlation with the corresponding pulse rates (Fig. 2).

The mean (×10<sup>-3</sup> mm<sup>2</sup>/s) interslice ADC values were 0.44 ± 0.27 in the left lobe in the preloaded study, 0.25 ± 0.19 in the right lobe in the preloaded study, 0.48 ± 0.22 in the left lobe in the postloaded study, and 0.27 ± 0.19 in the right lobe in the postloaded study. The difference between the values in the left and right lobes was statistically significant in both the pre- and postloaded studies (*P* = 0.006 and *P* < 0.001, respectively). On the other hand, the difference between the values of the pre- and postloaded studies was not significant in the left lobe or the right lobe (*P* = 0.19 and *P* = 0.44, respectively) (Table 1).

In visual evaluations, the left lobe showed a tendency to display a lower signal than the right lobe. This finding became more prominent in the postloaded images (Fig. 3). The grades of subcardiac signal loss in the postloaded images were significantly lower than the grades for the preloaded images (*P* < 0.001). Among the preloaded images, 33 slices were categorized as grade 1, with 45 and 12 slices grouped into grades 2 and 3, respectively. In contrast, in the postloaded images grades 1, 2, and 3 included 11, 39, and 40 slices, respectively (Table 2).

**Discussion**

Some authors have reported that malignant hepatic tumors have lower ADCs than benign lesions.<sup>9,10</sup>



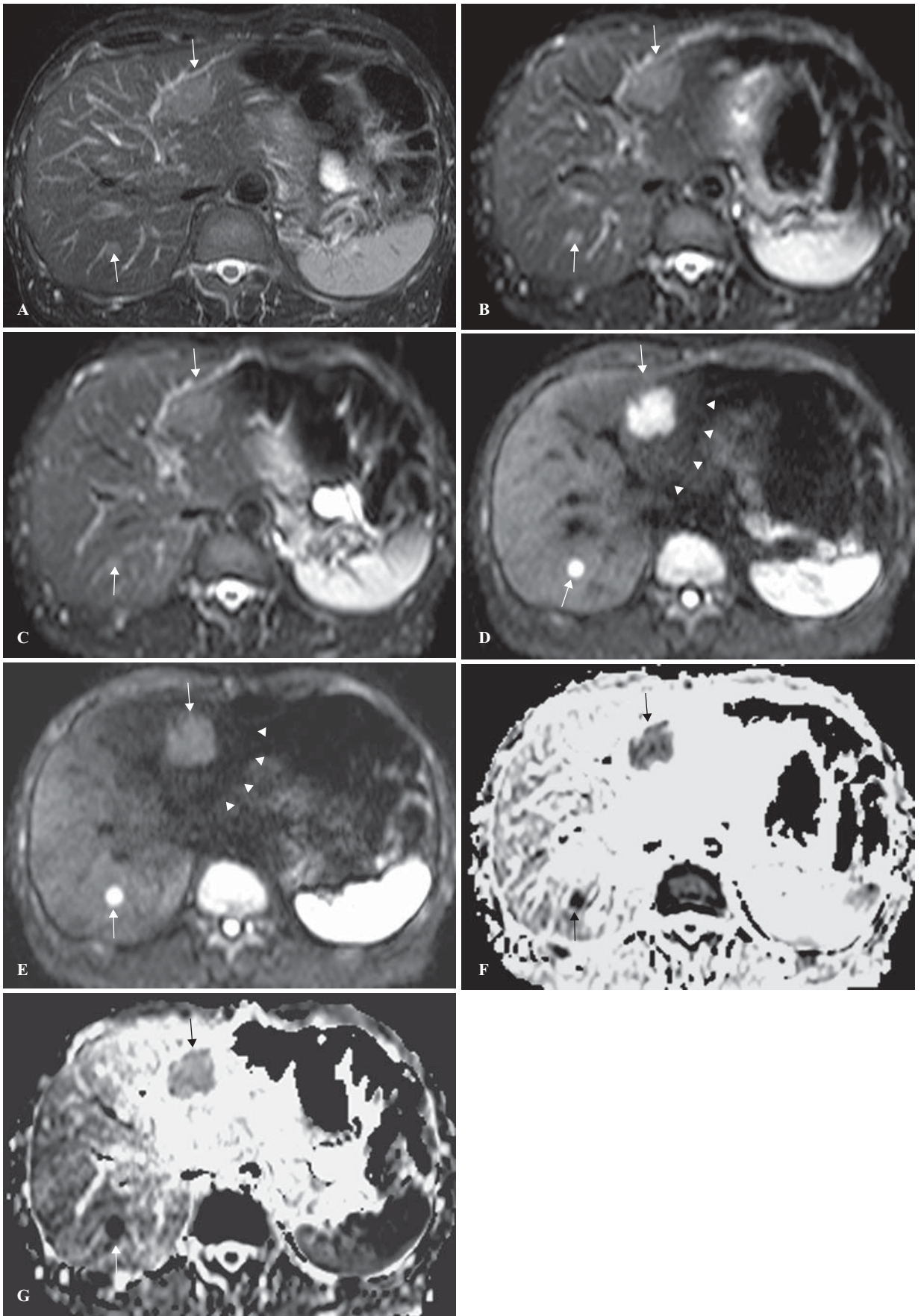


**Fig. 3.** **A** T2-weighted turbo spin echo (T2-TSE) (TR/TE 4468/90). **B** Preloaded T2-weighted echoplanar image with sensitivity encoding (SENSE-EPI) (TR/TE 1600/73,  $b = 0$ ). **C** Postloaded SENSE-EPI (TR/TE 1600/73,  $b = 0$ ). **D** Preloaded diffusion weighted image with SENSE (SENSE-DWI) (TR/TE 1600/73,  $b = 500$ ). **E** Postloaded SENSE-DWI (TR/TE 1600/73,  $b = 500$ ). **F** Preloaded ADC map. **G** Postloaded ADC map. The patient was a 56-year-old man with multiple liver metastases from colorectal cancer. Two metastatic tumors (*arrows*) are noted in the lateral and posterior segments. They show slightly more hyperintense signal than surrounding hepatic parenchyma both on T2-TSE (**A**), preloaded SENSE-EPI (**B**) and postloaded SENSE-EPI (**C**) (*arrows*). No clear differences can be pointed out between pre- and postloaded SENSE-EPIs. On the preloaded SENSE-DWI (**D**), these two metastases show more prominent signal and become more easily pointed out as compared with those on T2-TSE and SENSE-EPI. Note the signal drop of the lateral segment. This finding is the subcardiac signal loss. The margin of the lateral segment is indicated (*arrowheads*). Therefore, this artifact is classified as grade 2. On the other hand, the subcardiac signal loss becomes more significant on postloaded SENSE-DWI (**E**). The margin of the lateral segment is hardly seen (*arrowheads*). Therefore, this image is classified as grade 3. The metastasis in the lateral segment shows obviously lower signal than the lesion in the posterior segment in **E**. The results of ADC measurement in **F** and **G** are seen in the following: preloaded left lobe 2.95, preloaded right lobe 2.08, preloaded lateral segment tumor 1.26, preloaded posterior segment tumor 0.79, postloaded left lobe 3.76, postloaded right lobe 2.45, pos-loaded lateral segment tumor 2.91, and postloaded posterior segment tumor 0.95



Accordingly, ADC measurements are believed to have good potential for differentiating hepatic tumors. On the other hand, the correctness of ADC measurements in the liver has been in doubt because DWI is theoretically extremely sensitive to movement. MPG pulses, which bring specific contrast in DWI, suppress the signals of all moving proton with dephasing, including both diffusion phenomena and physiological motion. Therefore, the influence of physiological motion may appear as signal loss in diffusion-weighted images. For example, Murtz and her colleagues reported that cardiac gating with a discretely examined delay time was necessary for correct ADC measurement in the left hepatic lobes.<sup>7</sup> On the other hand, some authors have reported the feasibility of body DWI with the patient's breathing not restricted; however, this method has not yet been verified to be clinically useful.<sup>3</sup>

The ADC differences between the left and right lobes shown in this study are presumed to be due to the influence of cardiac motion, not histopathological differences in the measured hepatic parenchyma. The left lobe, which is located just below the heart, is probably shaken or distorted by cardiac motion during the systolic phase. Therefore, the MPG pulse used during the systolic phase depresses the signal of the left lobe to below normal values. This assumption supports the following findings

revealed in this study: (1) the subcardiac signal loss was more significant in postloaded images than in preloaded images, and (2) the influence of Buscopan was far stronger in the left lobe than the right lobe when the images were evaluated visually.

Our study also revealed that the influence of Buscopan on ADC measurement was not statistically significant, and there was no clear correlation between the left lobe ADC and the pulse rate. At first glance, these findings were inconsistent with the assumption mentioned in the previous paragraph. Theoretically, the left lobe ADC should rise with a faster pulse rate (more specifically, as the diastolic phase shortens). This contradiction is probably due to the influence of anatomical factors being too strong to mask the slight difference in pulse rate. However, during the actual image interpretation, image quality aggravation in the left lobe was obvious on the images after Buscopan administration.

Generally speaking, the diastolic phase in normal adults at rest is about 400 ms.<sup>11,12</sup> The duration of the binary MPG pulses (the time between the start of the first MPG pulse and the end of the second one) in the MR apparatus we used in this study was 60 ms. Therefore, it is theoretically possible to place the MPG pulses and EPI data acquisition during the diastolic phase using cardiac triggering. However, in practice, it is difficult to perform whole-liver DWI that satisfies the aforementioned preconditions with the simultaneous use of respiration gating and cardiac triggering. These are the reasons we set the number of excitations of SENSE-DWI to five. With an increased number of excitations, the probability of data acquisition during the diastolic phase would increase. However, the study revealed that our method did not have sufficient quality to measure correct ADCs in the left lobe.

During the visual evaluation, 79 of 90 slices were categorized as grade 1 or 2 in the preloaded study. In our postloaded study, however, only 40 of 90 slices were categorized as grade 1 or 2. We have empirically arrived at the knowledge that interpretation of hepatic DWI with slight signal loss is not difficult for trained diagnostic radiologists, provided the margin of the left lobe is visible. The high degree of compensating ability that is characteristic of the eyes and brains of humans is what enables this interpretative process. The image quality of the left lobe was thus assumed to be comparatively satisfactory for actual image interpretation, provided Buscopan was not used. We are unable to reach a final conclusion about this issue, however, because the study was not aimed at assessing the detectability of actual hepatic lesions. Despite this, the practical use of hepatic DWI without cardiac triggering is feasible in clinical scenarios based on the premise that the visual evaluation

methods are established and that we do not rely entirely on ADC measurement.

This study had some limitations. The ADC measurement in the upper abdominal organs was far more incorrect than that in the brain. The hepatic ADCs measured in this study were markedly scattering not only between lobes but also among the slices from each patient. Therefore, repeated measurements and averaging of the ADCs were necessary for correct evaluation of the hepatic parenchyma.<sup>7</sup> The method performed in this study was different from the ideal one. The b-factor selected in our study was too low to obtain precise ADCs. However, the aim of this study was not to measure the correct ADC of hepatic parenchyma but to demonstrate the difficulty of correctly measuring ADCs in the left lobe and the unfavorable influence of Buscopan administration. Probably the phenomenon described herein is always observed with any abdominal DWI without cardiac triggering despite the value assigned to the b factor.

## Conclusions

The ADCs of the left lobe were higher than those of the right lobe, and Buscopan administration enhanced this difference. We assume that this phenomenon is due to cardiac pulsation. For hepatic DWI without cardiac triggering, therefore, the visual evaluation needs to be given priority over ADC measurement.

## References

- Nasu K, Kuroki Y, Kuroki S, Murakami K, Nawano S, Moriyama N. Diffusion-weighted single shot echo planar imaging of colorectal cancer using a sensitivity-encoding technique. *Jpn J Clin Oncol* 2004;34:620–6.
- Kuroki Y, Nasu K, Kuroki K, Murakami K, Hayashi T, Sekiguchi R, et al. Diffusion weighted imaging of breast cancer with the apparent diffusion coefficient value. *Magn Reson Med Sci* 2004;3:79–85.
- Takahara T, Imai Y, Yamashita T, Yasuda S, Nasu S, Van Cauteren M. Diffusion weighted whole body imaging with background body signal suppression (DWIBS): technical improvement using free breathing, STIR and high resolution 3D display. *Radiat Med* 2004;22:275–82.
- Nasu K, Kuroki Y, Nawano S, Kuroki S, Tsukamoto T, Yamamoto S, et al. Hepatic metastases: diffusion-weighted sensitivity-encoding versus SPIO-MRI-enhanced MR imaging. *Radiology* 2006;239:122–30.
- Stejskal EO, Tanner JE. Spin echoes in the presence of a time-dependent field gradient. *J Chem Phys* 1965;42:288–92.
- Haake EM, Brown RW, Thompson MR, Venkatesan R. Random walk, relaxation and diffusion. In: Haake EM (ed) *Magnetic resonance imaging: physical principles and sequence design*. New York: Wiley; 1999. p. 619–36.
- Murp P, Flacke S, Traber F, van den Brink JS, Gieseke J, Schild HH. Abdomen: diffusion-weighted MR imaging with pulse-triggered single-shot sequence. *Radiology* 2002;224:258–64.
- Xing D, Papadakin NG, Haung CLH, Lee VM, Carpenter TA, Hall LD. Optimized diffusion-weighting for measurement of apparent diffusion coefficient in human brain. *Magn Reson Imaging* 1997;15:771–84.
- Ichikawa T, Haradome H, Hachiya J, Nitatori T, Araki T. Diffusion-weighted MR imaging with a single-shot echoplanar sequence: detection and characterization of focal hepatic lesions. *AJR Am J Roentgenol* 1998;170:397–402.
- Kim T, Murakami T, Takahashi S, Hori M, Tsuda K, Nakamura H. Diffusion-weighted single-shot echoplanar MR imaging for liver disease. *AJR Am J Roentgenol* 1999;173:393–8.
- Josephson ME. Electrophysiologic investigation: general concept. In: Josephson ME (ed) *Clinical cardiac electrophysiology technique and interpretation*, 2nd ed. Philadelphia: Williams & Wilkins; 1993. p. 22–70.
- Denes P, Wu D, Dhingra R, Pietras RJ, Rosen KM. The effects of cycle length on cardiac refractory periods in man. *Circulation* 1974;49:32.